Appendix

Computing Albedo (Sensitivity and) Feedback

Figures A1a-d illustrates the albedo sensitivity concept and magnitude calculation from regression of inter annual anomalies. In this example, values from the grid cells nearest two representative GC-Net sites are selected to illustrate the differences between the ablation area represented by the JAR1 AWS location, not the AWS data and the accumulation area represented by the Summit AWS location. Over most of the accumulation area, temporal detrending changes the sign of the regression from positive (expected) to negative.
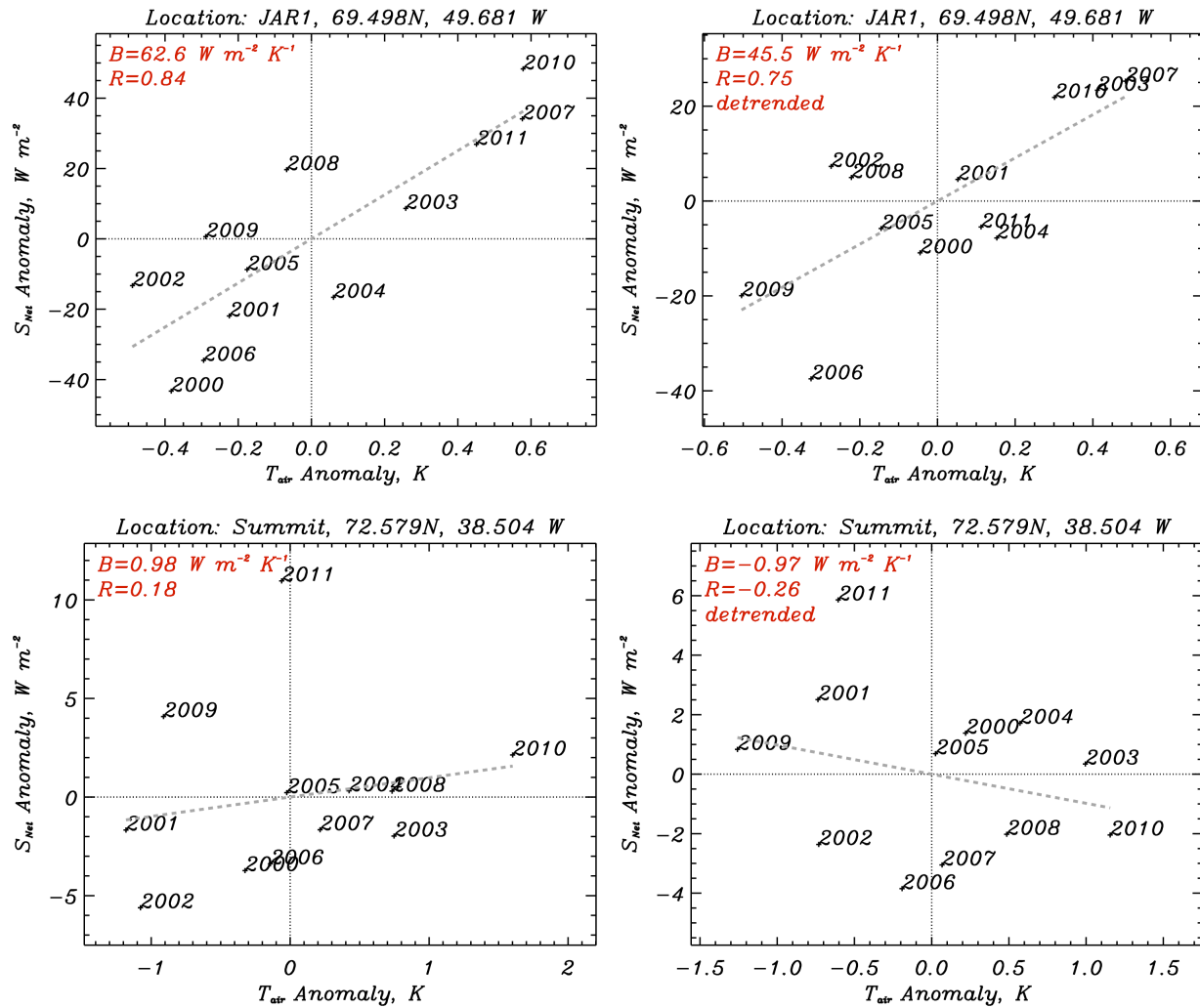
Fig. A1. Examples of albedo feedback calculated by regression of inter annual anomalies. The dashed grey line indicates the regression slope that quantifies the magnitude of the feedback.

Albedo sensitivity to T_{Air} (not shown in the form above) is calculated by the *same* concept of statistical regression between inter annual anomalies.

Effect of Temporal Detrending on Calculating Albedo Sensitivity

Temporal detrending prior to anomaly calculation leads to differences in calculated albedo sensitivity to temperature and albedo feedback. Box et al. (TCD, 2012) feature the detrended results because they believe the detrended results more closely represent the sensitivity and feedback processes.

Detrending enhances the positive sensitivity while decreasing the negative sensitivity. The reason for this has to do with the fact that the albedo decreasing trend is stronger than the temperature increasing trend. Nonetheless, evidence of positive sensitivity remains in the non-detrended data.
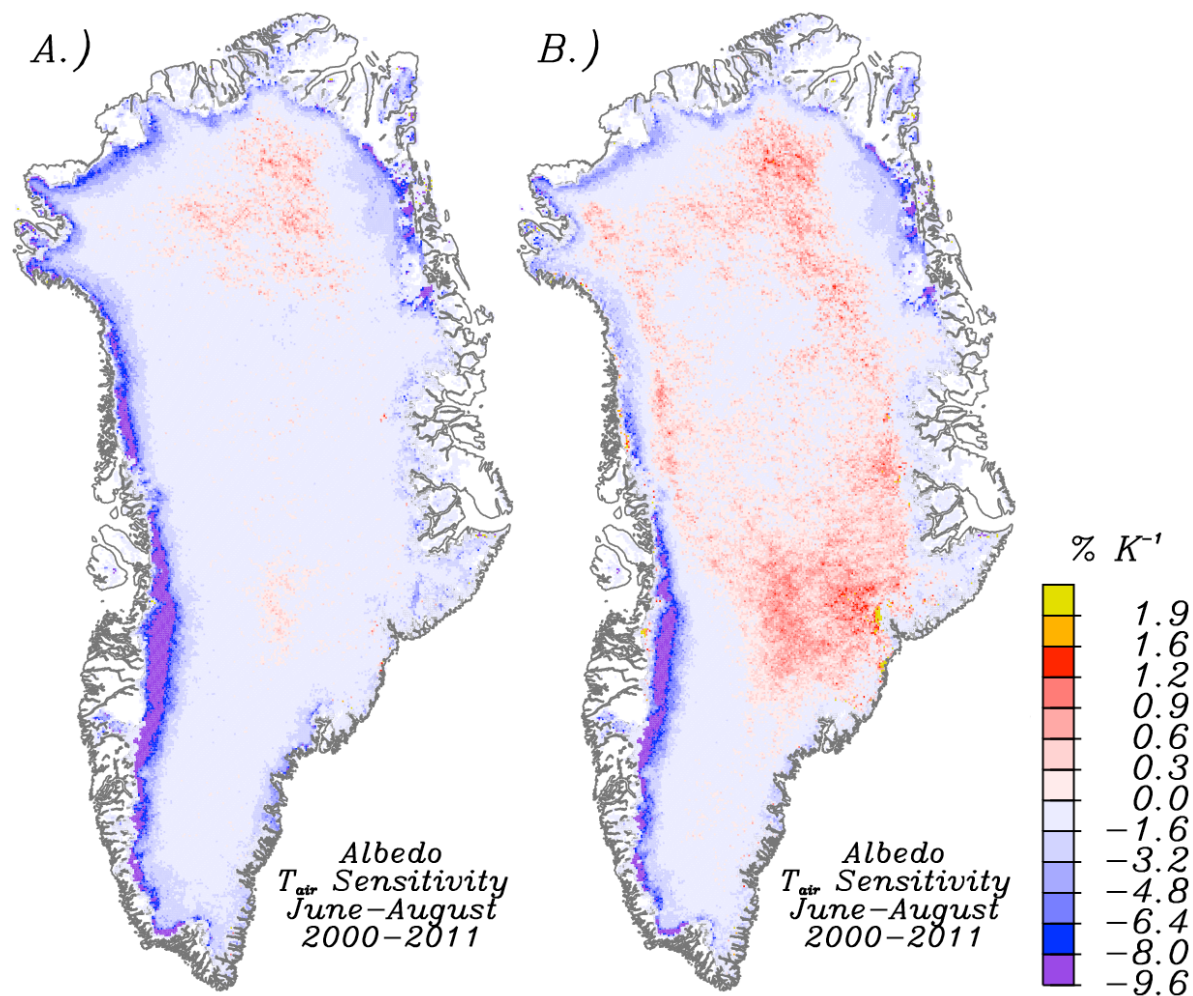

Fig. A2. (A) (a) summer spatial patterns of ice sheet albedo sensitivity based on MODIS albedo observations and MAR simulations of T_{air} (B). Same as A but with temporal detrending of albedo and temperature prior to regression. The positive scale is 1/3rd that of the positive scale. The regressions are detrended to minimize spurious correlation.

When MODIS albedo are replaced with albedo calculations from MAR, the positive sensitivity regions are stronger. The effect of temporal detrending has a weaker effect when using only MAR data.
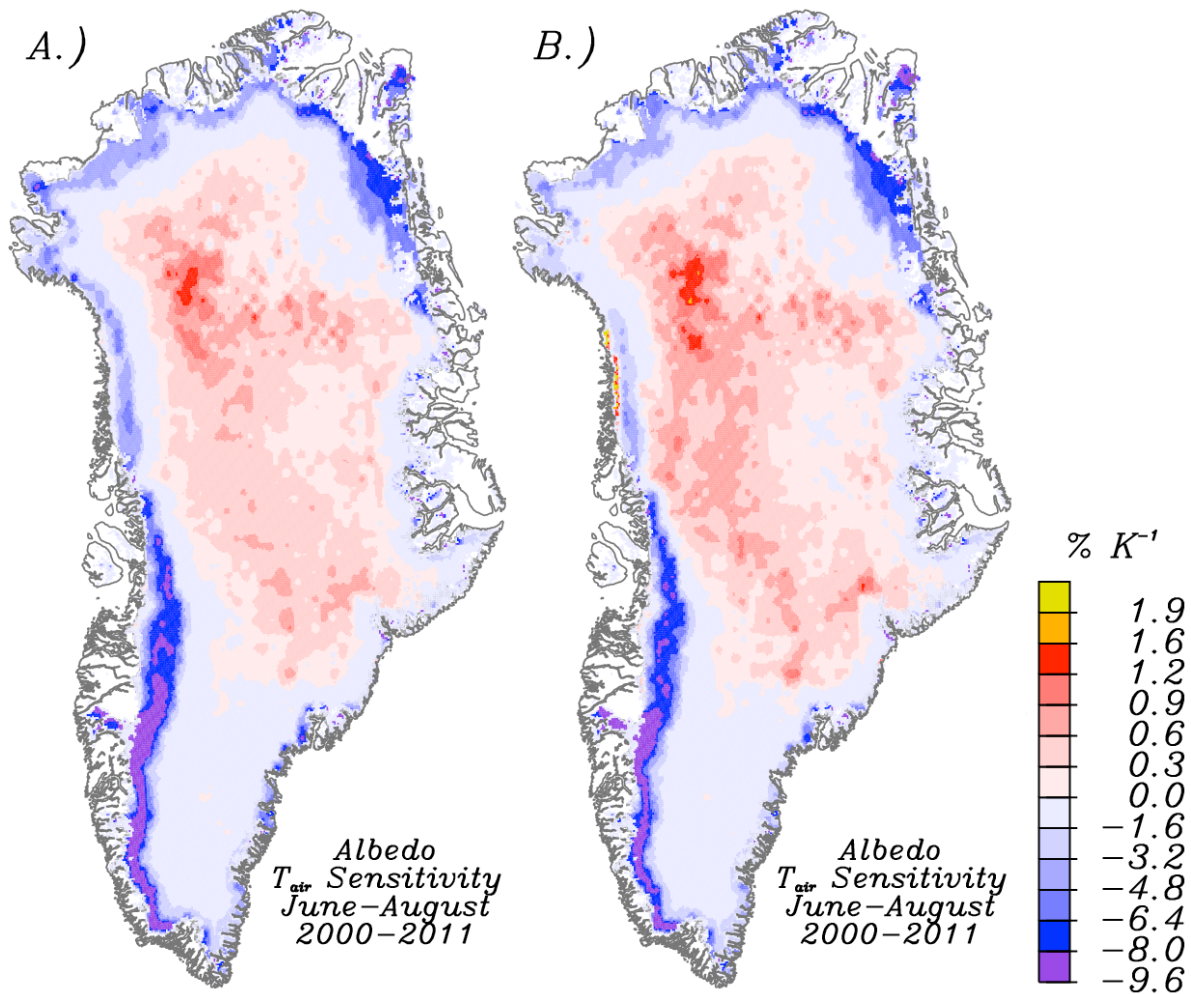

Fig. A3. Same as Fig. A2, but using albedo calculated by MAR. In this example, all data are from MAR.
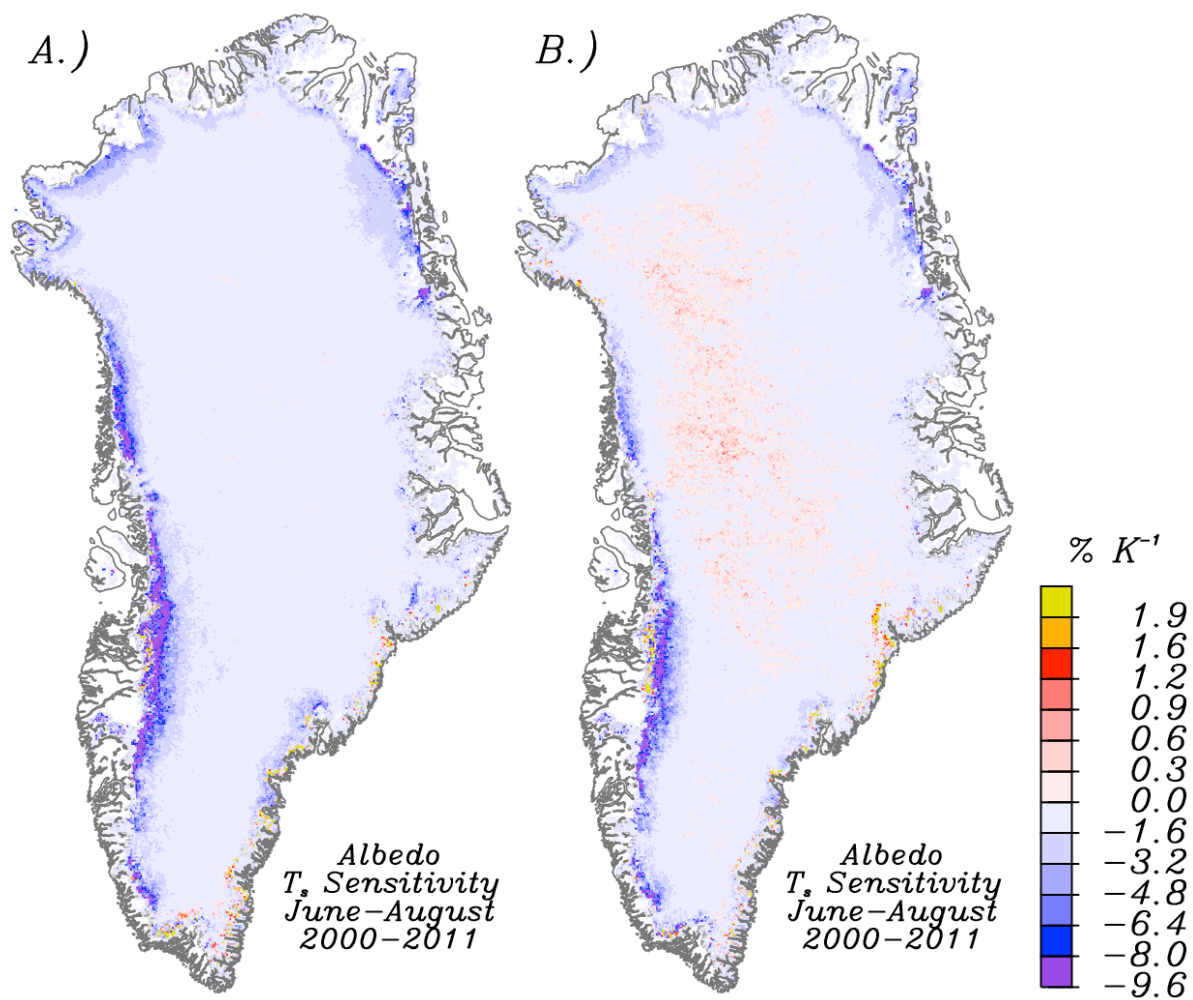
Fig. A4. Same as Fig. A2, but using MODIS MOD11A1 land surface temperature instead of near-surface air temperatures calculated by MAR.

Another illustration of the impact of temporal detrending is made in Figs. A5a,b where some positive sensitivity is evident in the non-detrended data.
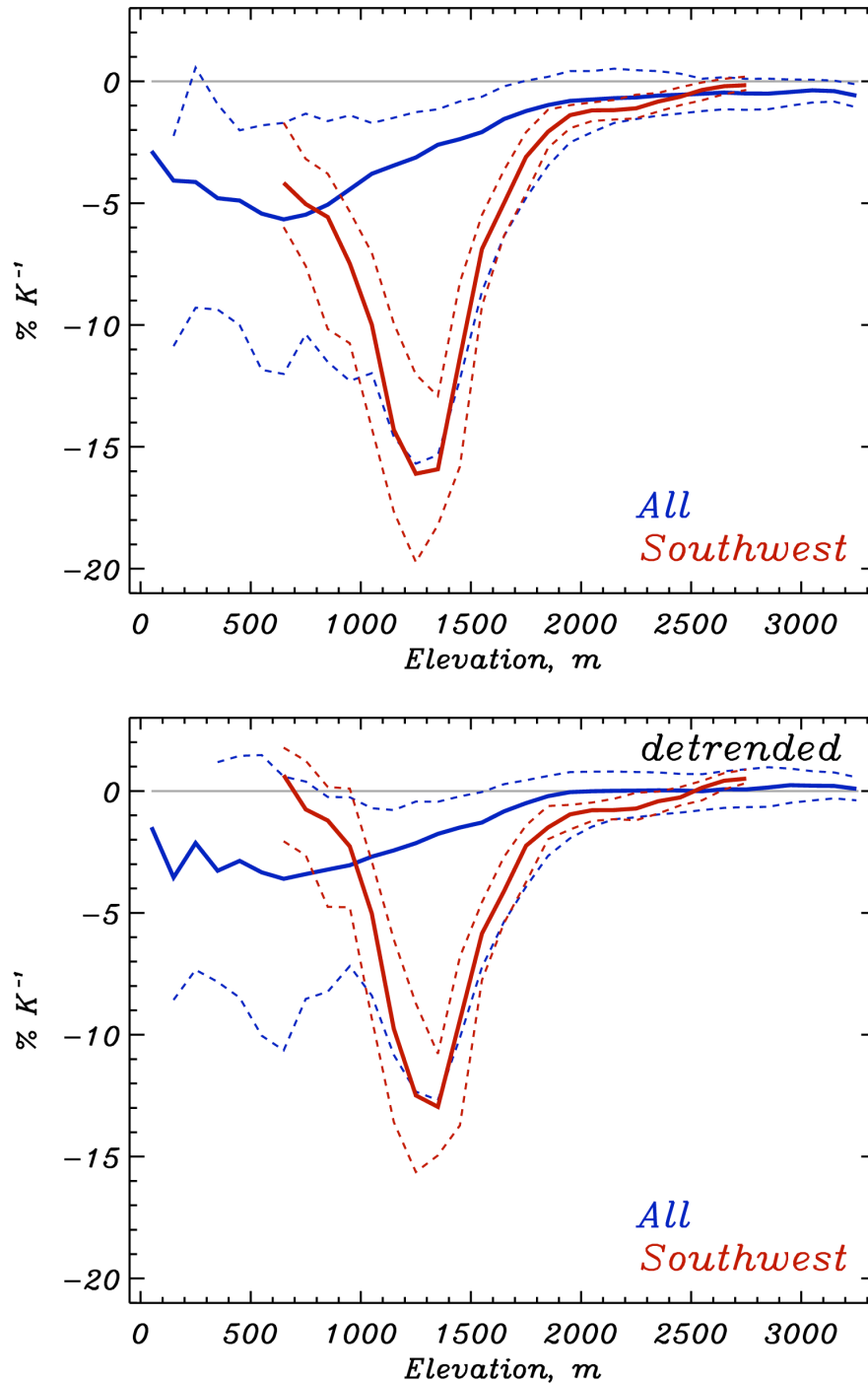

Fig. A5. (a, top) Elevation profile of calculated MODIS albedo sensitivity to MAR simulations of T_{air}. The solid line represents the median while the dashed lines represent the 95th and 5th percentiles in the distribution. (b, bottom) same as (a, top) but with temporal detrending prior to regression. The southwest region is west of the ice divide, in the 2 degree latitude zone north of 66 degree N latitude.
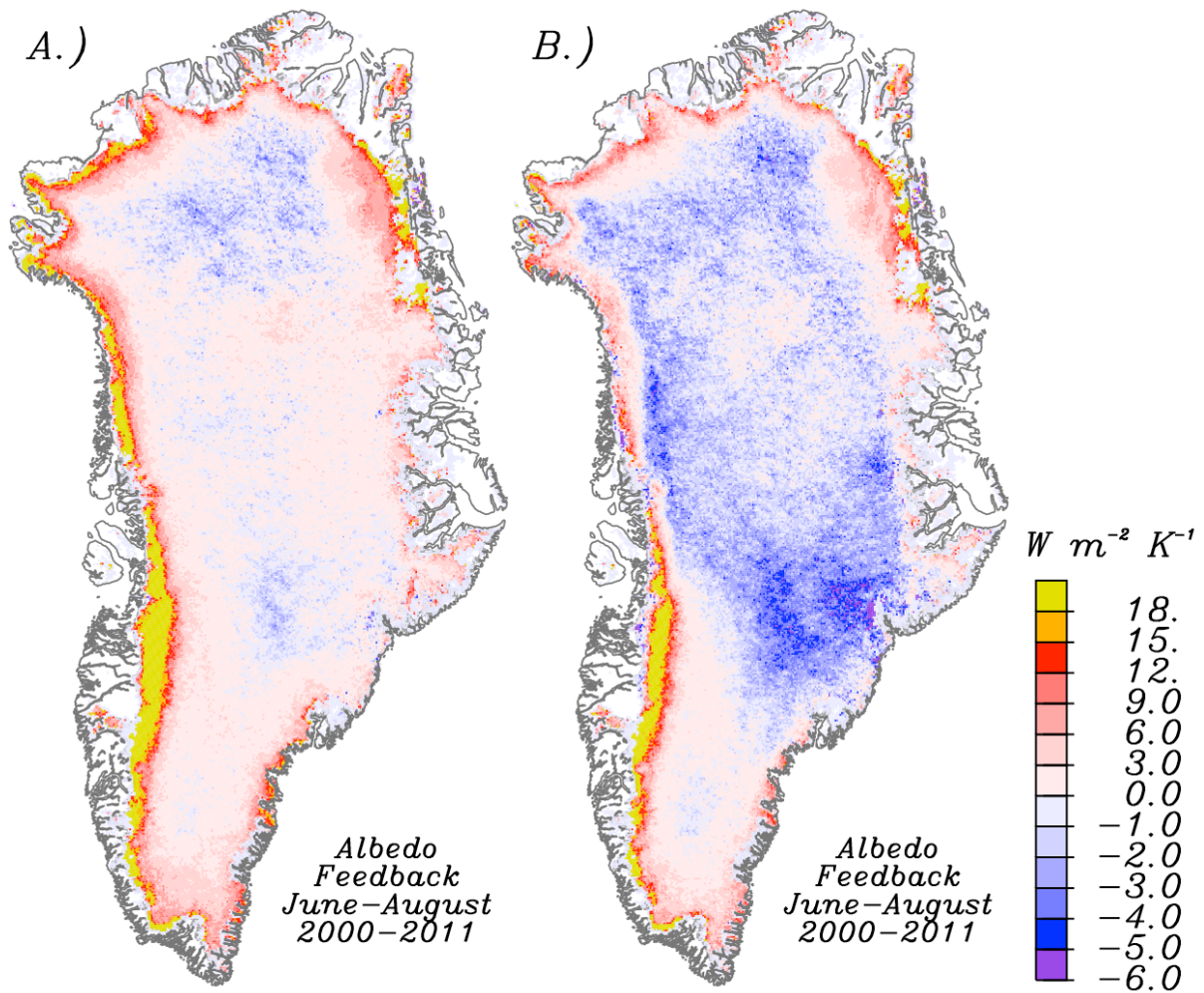
Fig. A6. (A) (a) summer spatial patterns of ice sheet albedo feedback based on MODIS albedo observations and MAR simulations of S↓ and T_{air} (b). The negative scale is 1/3rd that of the positive scale. The regressions are detrended to minimize spurious correlation.

When MODIS albedo are replaced with albedo calculations from MAR (Figs A7a,b), the negative feedback areas are stronger in magnitude. The core of the negative correlation is co-located where MAR output indicates the strongest correlation between snowfall and air temperature (Fig. 9a), indicating increased snowfall with increasing temperature is a key source of the negative feedback. The effect of temporal detrending has a weaker effect when using only MAR data.
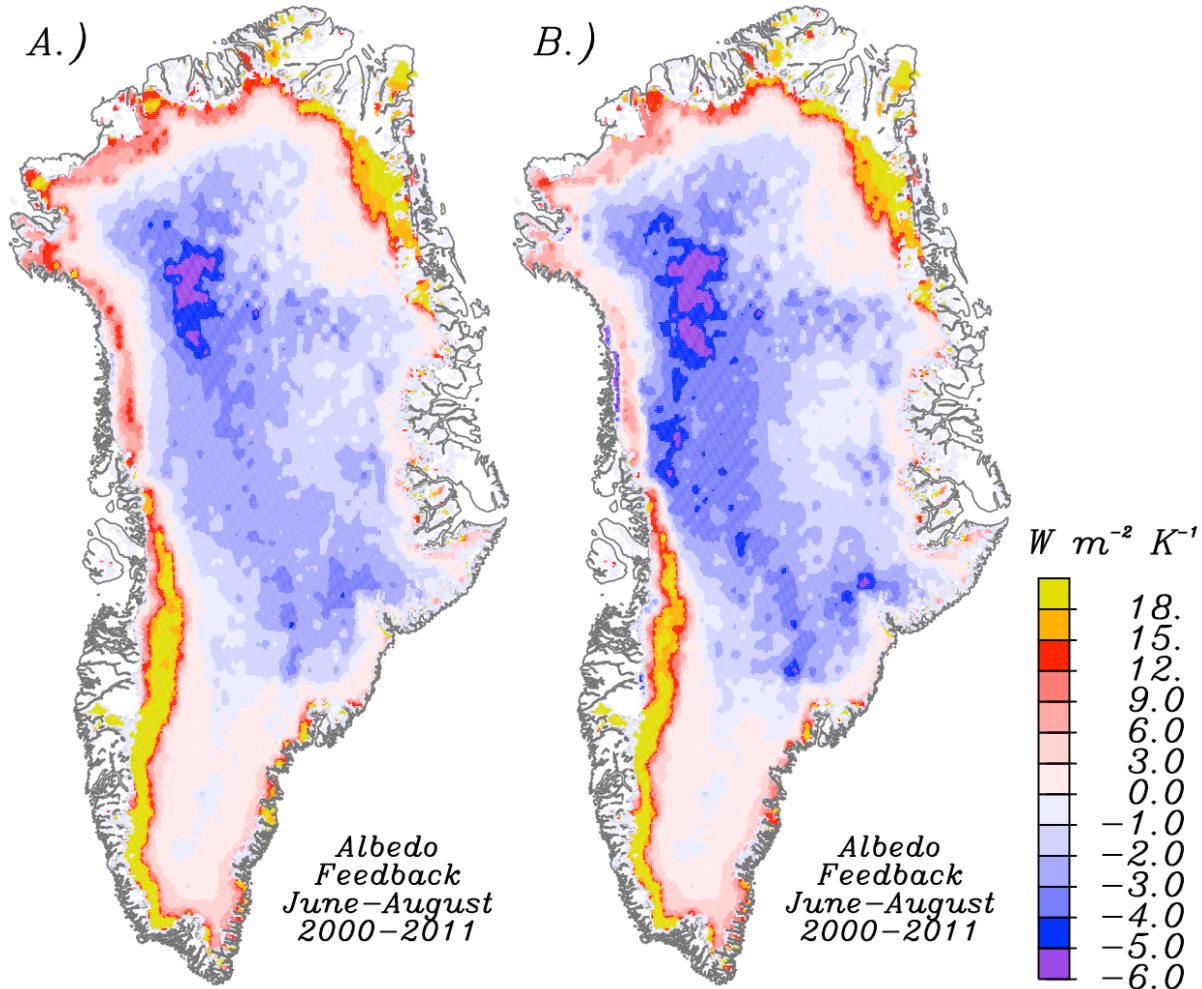

Fig. A7. Same as Fig. A5, but using albedo calculated by MAR. In this example, all data are from MAR.

Another illustration of the impact of temporal detrending is made in Figs. A8a,b where some negative feedback is evident in the non-detrended data.
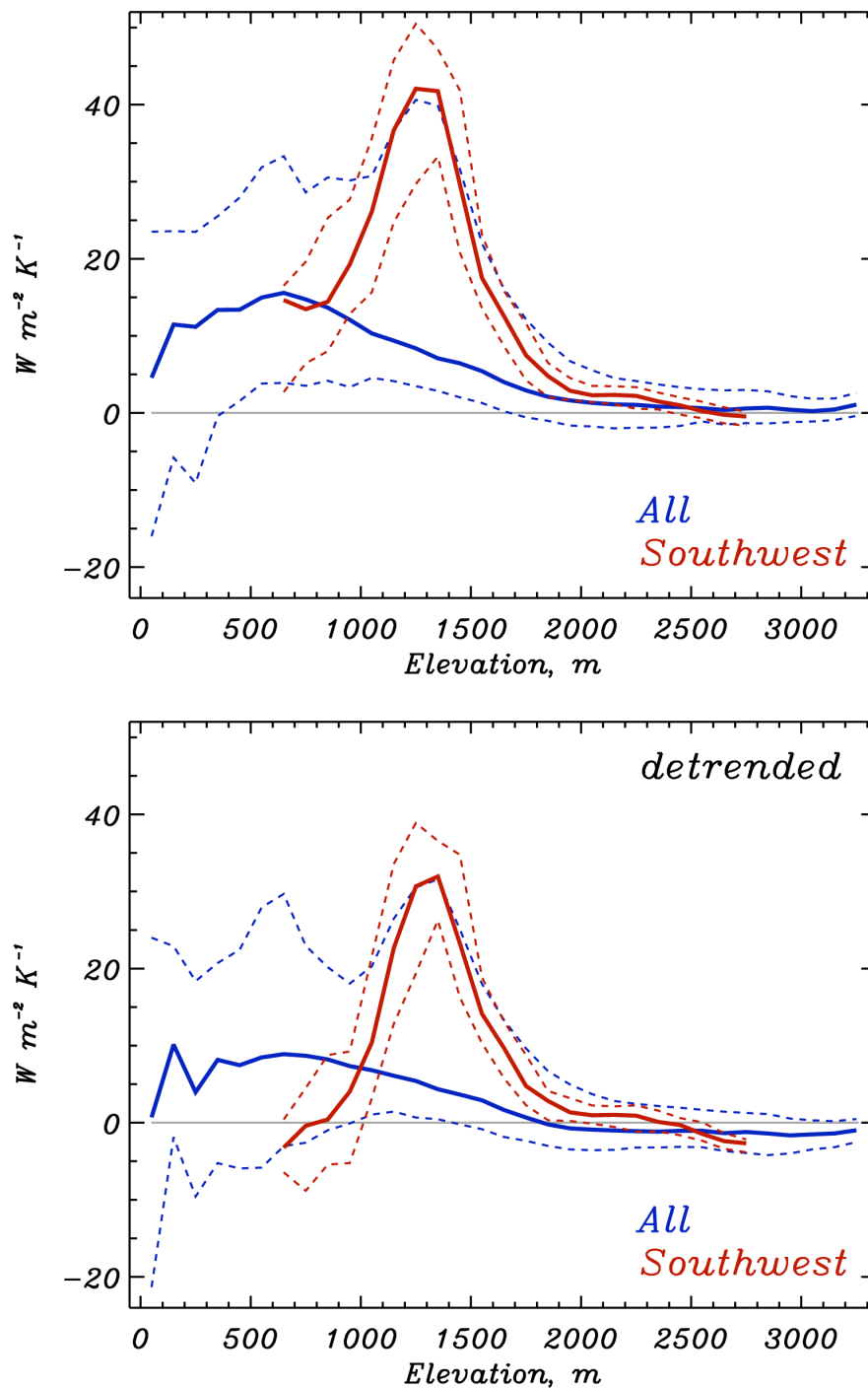

Fig. A8. (a, top) Elevation profile of calculated albedo feedback based on MODIS albedo observations and MAR simulations of $S\downarrow$ and T_{air}. The solid line represents the median while the dashed lines represent the 95th and 5th percentiles in the distribution. (b, bottom) same as (a, top) but with temporal detrending prior to regression.

When the MODIS MOD10A1 data are not temporally detrended, the area of positive albedo sensitivity to air temperature is less than when the data are detrended (Figs. A9a,b). Detrending has the effect of allowing anomalies to assert their impact on the albedo variability more clearly than without detrending.
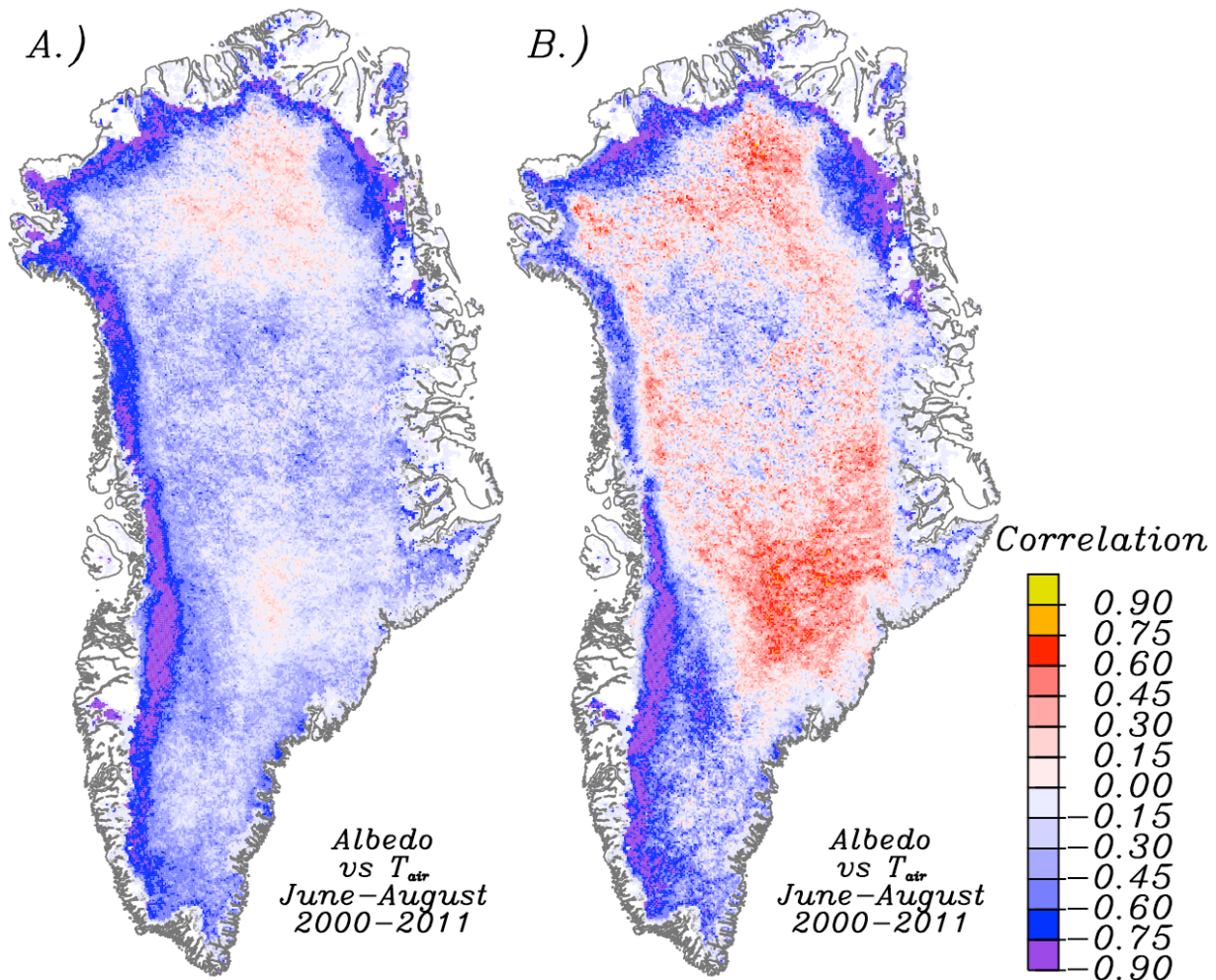

Fig. A9. (A) summer spatial patterns of not temporally-detrended ice sheet of MODIS MOD10A1 albedo and MAR simulations of T_{air} . (B). Same as A but with temporal detrending of albedo and temperature prior to regression.

Testing whether the somewhat unexpected positive correlation regions (positive albedo sensitivity with temperature) is real, MAR simulated albedo is compared with MAR simulated air temperature in Figs. A10a,b. In this case, the positive correlation area dominating in detrended and not-detrended results supports the hypothesis that in warmer climates, there is a tendency for higher albedo in the area of the ice sheet where there is little melting. Fig. 10A from the main article confirms more simulated snowfall in warmer years that supports the patterns evident here.
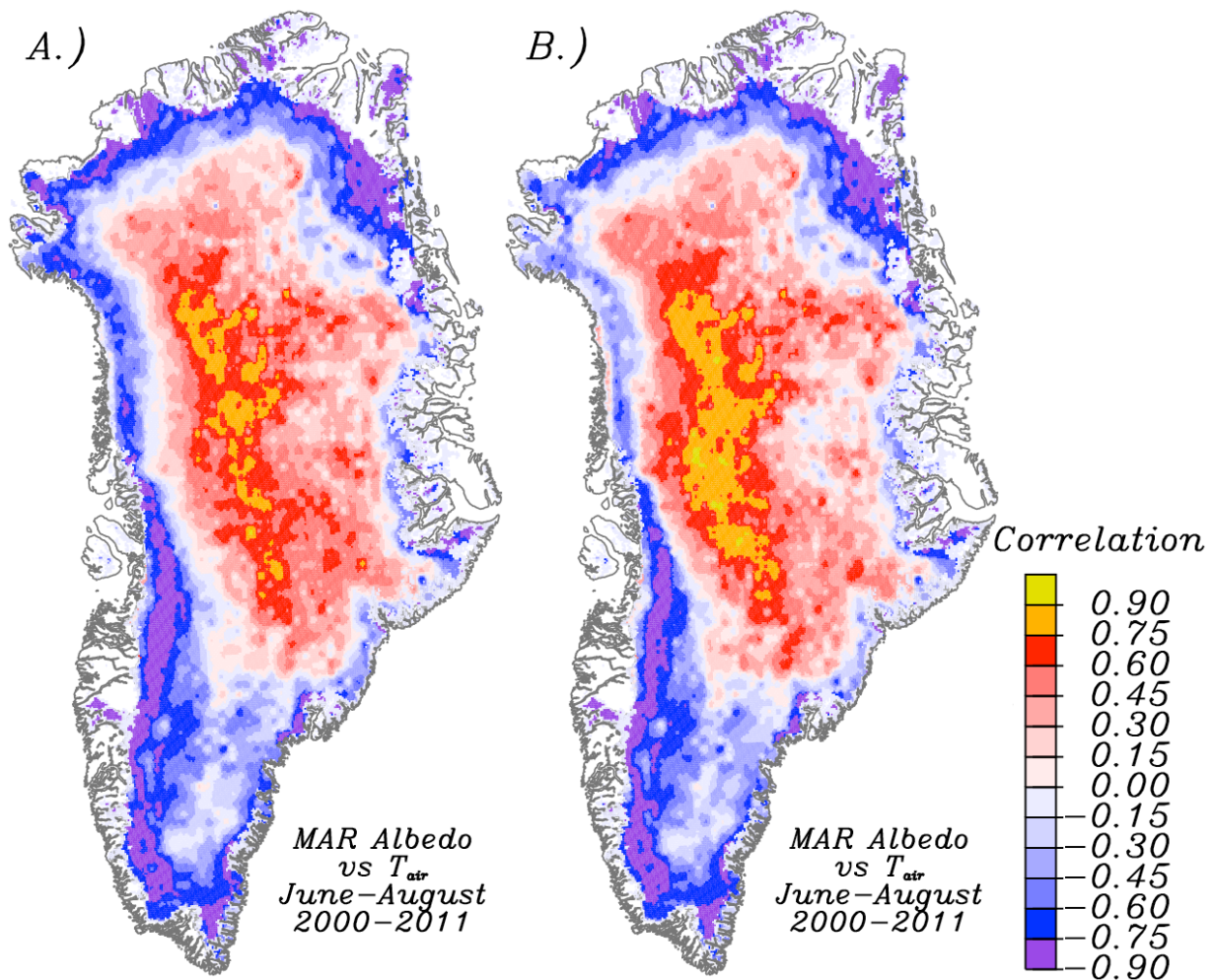

Fig. A10. (A) summer spatial patterns of not temporally-detrended ice sheet MAR simulations of albedo and T_{air} . (B) Same as A but with temporal detrending of albedo and temperature prior to regression.
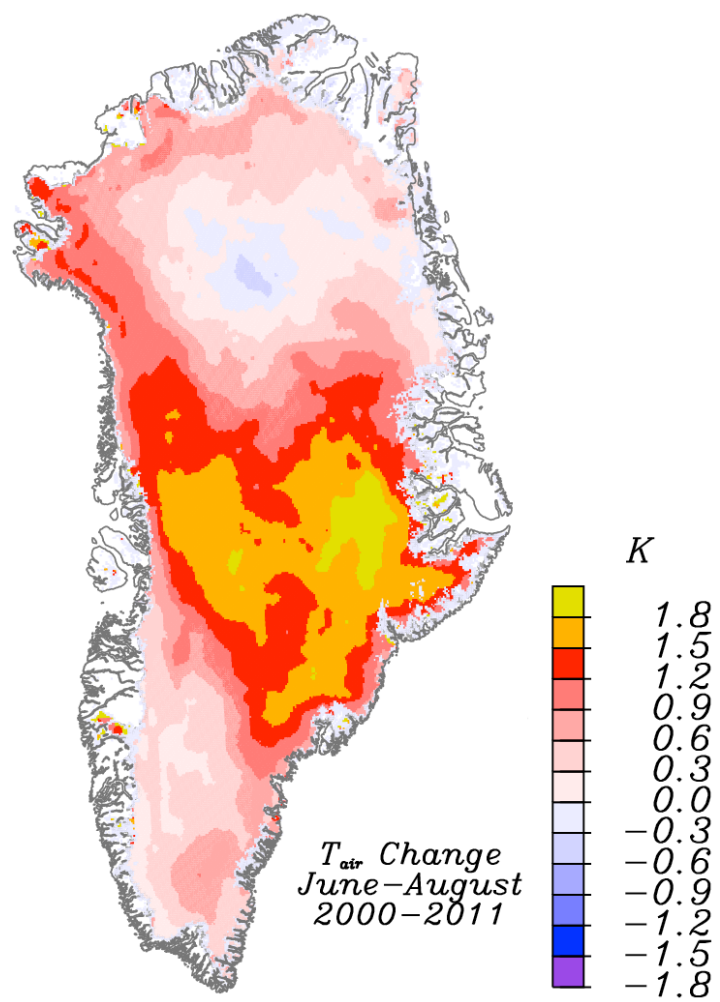
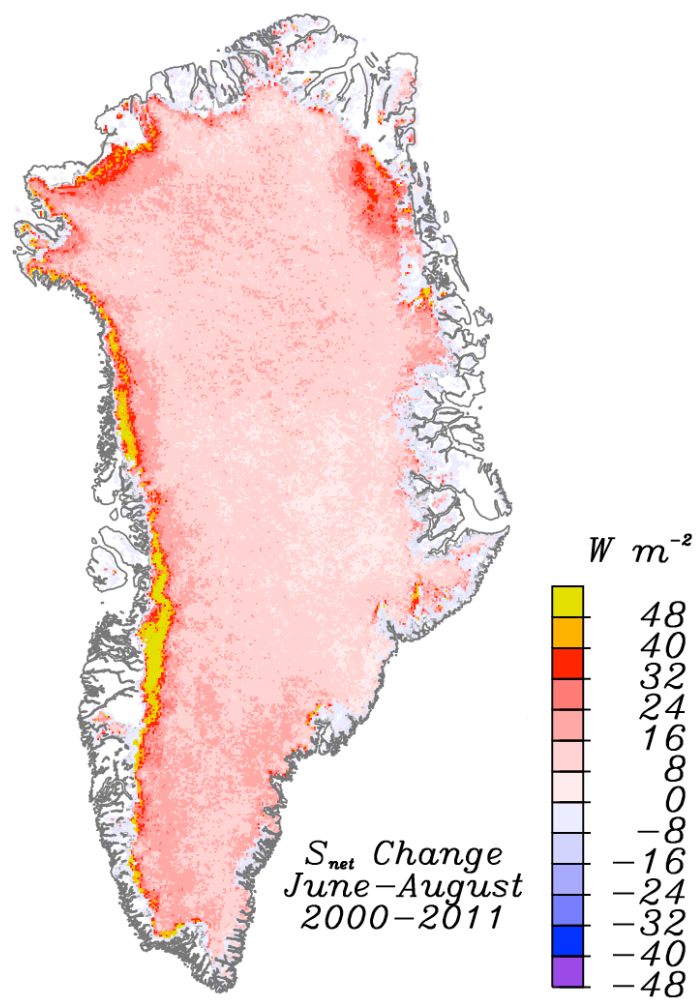Fig. A11. Summer spatial patterns of MAR simulated T$_{air}$ change 2000-2011.

Fig. A12. Summer spatial patterns of MAR simulated S_{net} change 2000-2011.